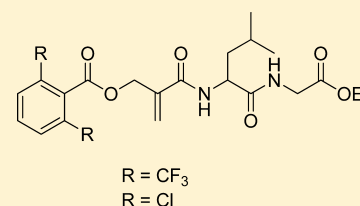


Studies toward Novel Peptidomimetic Inhibitors of Thioredoxin–
Thioredoxin Reductase SystemSzymon Kłossowski,^{†,§} Angelika Muchowicz,^{‡,§} Małgorzata Firczuk,[‡] Marta Świech,[‡] Adam Redzej,[†]
Jakub Golab,^{*,‡} and Ryszard Ostaszewski^{*,†}[†]Institute of Organic Chemistry, Polish Academy of Sciences, Kasprzaka 44/52, 01-224 Warsaw, Poland[‡]Department of Immunology, Center of Biostructure Research, Medical University of Warsaw, Banacha 1A, F building, 02-097 Warsaw, Poland

S Supporting Information

ABSTRACT: Thioredoxins (Trx) are ubiquitous multifunctional low-molecular weight proteins that together with thioredoxin reductases (TrxR) participate in the maintenance of protein thiol homeostasis in NADPH-dependent reactions. An increasing number of data reveal that the Trx–TrxR system is an attractive target for anticancer therapies. In this work, we have elaborated a new and simple synthetic approach employing Ugi reaction to synthesize several new inhibitors of this system. The influence of various electrophilic fragments of this new class of compounds on the inhibition of the Trx–TrxR system was evaluated. As a result, a new compound **19a** (SK053), which inhibits the activity of the Trx–TrxR system and exhibits antitumor activity, was obtained. Biologic analyses revealed that **19a** inhibits induction of NF- κ B and AP-1 and decreases H₂O₂ scavenging capacity in tumor cells. Altogether, we show that **19a** is a novel potential antitumor peptidomimetic inhibitor that can be used as a starting compound for further optimization.



1. INTRODUCTION

Thioredoxins (Trx) are ubiquitous multifunctional low-molecular weight proteins that together with thioredoxin reductases (TrxR) participate in the maintenance of protein thiol homeostasis in nicotinamide adenine dinucleotide phosphate (NADPH)-dependent reactions.¹ Trx provide reducing equivalents to a number of target molecules including ribonucleotide reductase, participate in scavenging reactive oxygen species (ROS) primarily by reducing peroxiredoxins, and regulate the activity of various transcription factors, such as p53,² HIF-1, nuclear factor κ B (NF- κ B), and activating protein-1 (AP-1)^{3,4} as well as protein tyrosine phosphatases, such as phosphatase and tensin homologue deleted on chromosome ten (PTEN)⁵ or Cdc25.⁶ The influence of Trx on some transcription factors is mediated by reduction of a redox factor, which has a DNA repair endonuclease activity.⁴ Two similar Trx systems exist in eukaryotic cells: a cytosolic one consisting of a 12 kDa Trx-1 and homodimeric seleno-protein TrxR-1 as well as mitochondrial, which includes Trx-2 and TrxR-2.⁷

Trx belong to oxidoreductases, a class of enzymes catalyzing redox reactions. Trx perform reduction of disulfide bonds in proteinaceous substrates. X-ray crystallography,^{8,9} protein nuclear magnetic resonance (NMR),¹⁰ and biochemical investigations¹¹ jointly contributed to the elucidation of the mechanism of the reaction catalyzed by Trx. The three-dimensional structure of Trx revealed a common folding unit named the Trx fold and the active site formed by two Cys residues, which belong to the conserved CXXC sequence motif. In human Trx-1, the motif comprises Cys32-Pro-Gly-Cys35. It is believed that the reaction catalyzed by Trx is initiated by a direct nucleophilic attack of the Cys32 thiolate on a sulfur atom

of a substrate disulfide, resulting in the formation of the transient intermolecular disulfide bond. Next, the second nucleophilic attack of the Cys35 occurs, which generates a dithiol in a proteinaceous substrate and a disulfide in Trx. To enable the next cycle of the reduction, the Trx has to be enzymatically reduced by NADPH-dependent TrxR.⁷ Human TrxR are homodimeric enzymes containing a seleno-cysteine (Sec) residue at the protein C terminus. This residue belongs to the conserved Gly-Cys-Sec-Gly- sequence motif and plays an essential role in catalysis of Trx reduction.¹² The Sec residue is a strong nucleophile and thus has been shown to be a molecular target for electrophilic compounds such as antitumor quinols.¹³

The Trx–TrxR system plays a distinct functional role among cellular antioxidants mainly due to its capacity to reduce other proteins by cysteine thiol-disulfide exchange. By reducing peroxiredoxins or glutathione peroxidase 3 that regulate hydrogen peroxide (H₂O₂) levels, Trx provide a link between major antioxidant systems. Trx can also reduce methionine sulfoxide reductase, quench singlet oxygen (¹O₂), and act as hydroxyl radical ([•]OH) scavengers.^{13–15} Recent observations indicate that Trx are the only cellular enzymes that can participate in protein denitrosylation.¹⁶ Inhibition of the Trx–TrxR system can therefore lead to a profound imbalance in the redox state that can ultimately lead to apoptosis. Additionally, Trx-1 can directly protect cells from apoptotic signaling through binding to apoptosis signal-regulating kinase (ASK1),¹⁷ a member of the mitogen-activated protein (MAP)

Received: June 8, 2011

Published: December 1, 2011

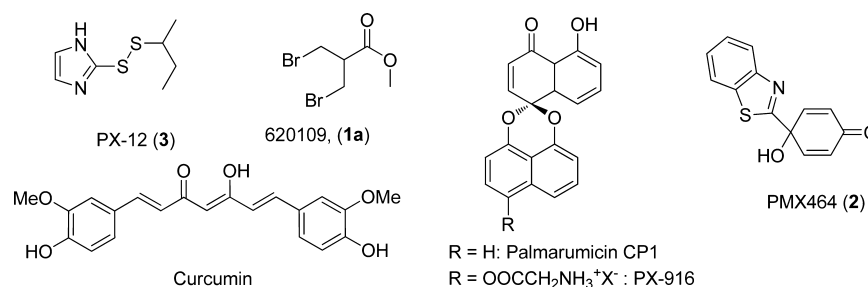


Figure 1. Compound 3 and electrophilic inhibitors of the Trx–TrxR system.

kinase family, or via inhibition of procaspase 3 processing and activation.¹⁸

Increased levels and activity of Trx are found in many different tumor types including solid tumors, leukemias, and lymphomas¹⁹ and are associated with more aggressive tumor progression and worse prognosis.^{20,21} Trx may facilitate tumor progression through growth-promoting and antiapoptotic functions.²² At later stages of tumor progression, Trx may promote angiogenesis through increased activity of hypoxia-inducible factor (HIF-1) and secretion of vascular endothelial growth factor (VEGF) or metastasis by modulating the activity of matrix metalloproteinases (MMP).^{23,24} Moreover, increased Trx levels have been associated with tumor resistance to chemotherapeutics, such as cisplatin, docetaxel, mitomycin C, etoposide, or doxorubicin.^{25–28}

All of these biological activities indicate that the Trx–TrxR system is an attractive target for anticancer treatment. Indeed, several inhibitors of Trx have been developed, and one, PX-12 (3),²⁹ progressed to phase II clinical trials as an anticancer agent. Compound 3 is a substituted 2-imidazolyl disulfide that thioalkylates cysteine residues of Trx, especially Cys73, which is thioalkylated irreversibly. When Cys73 is alkylated, Trx cannot be reduced, which leads to its inactivation.^{29,30} Phase I clinical trials revealed, however, some undesired features of disulfides such as pneumonitis induction as well as pungent, unpleasant, garlic-like odor of thiol methabolites.³¹ Other Trx–TrxR system inhibitors include naphthoquinone spiroketal compounds [such as palmarumycin CP1, PX-916,^{32,33} gold compounds,³⁴ the organotellurium analogue of vitamin E,³⁵ or PMX464 (2, previously AW464)].³⁶ Moreover, histone deacetylase inhibitor, suberoyl anilide hydroxamic acid (SAHA), which is approved for the treatment of cutaneous T-cell lymphoma, up-regulates the expression of an endogenous Trx inhibitor–Trx-binding protein 2 (TBP-2).³⁷

Considering the features of described inhibitors of the Trx–TrxR system, we designed novel compounds with a peptidomimetic scaffold that could target these enzymes to become potential anticancer therapeutics.

2. RESULTS AND DISCUSSION

A characteristic feature of the majority of known inhibitors of Trx system is the presence of an electrophilic fragment, which can covalently interact with cysteines or Sec in the active site of Trx or TrxR (Figure 1).^{38,39} Compound 2 has two electrophilic centers, and one of the proposed mechanisms of its action is based on a two-step thioalkylation of both cysteines of Trx within the active site by a single inhibitor molecule leading to a macrocyclic adduct.⁴⁰ A similar mechanism is also described for Mannich bases, which also exhibit high Trx system inhibiting activity.⁴¹ Considering these mechanisms, we hypothesized that

the presence of double nucleophilic center in Trx can be targeted by compounds that have two electrophilic groups. On the basis of this assumption, we also hypothesized that inhibition of Trx by 3-bromo-2-bromomethylpropionic acid methyl ester (1a)⁴² can be explained by the mechanism presented in Figure 2.

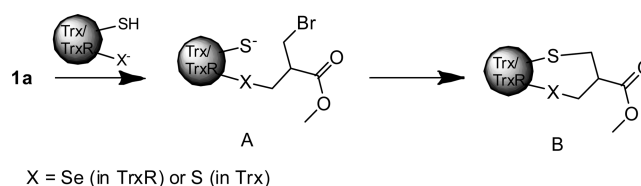


Figure 2. Putative alkylation of cysteines in Trx by 1a.

For the initial screening of the capacity of the intermediate compounds to inhibit the Trx–TrxR system, we have employed a coupled, Trx–TrxR-dependent insulin reduction assay.⁴³ Tested compounds were incubated for 30 min at 37 °C together with all other assay reagents, and the IC₅₀ values were designated (see the Experimental Section). As shown in Table

Table 1. Biologic Activities of 3 and Peptidomimetic Analogues of 1a and 1b

compd	IC ₅₀ ^a (μM)	LD ₅₀ ^b (μM)	
		EMT6	Panc02
3	12.3 ± 0.6	11.6 ± 0.6	3.9 ± 0.2
1a	1.2 ± 0.8	>50	>50
13	>50	ND ^c	ND
14a	>50	ND	ND
14b	>50	ND	ND
15	>50	ND	ND
1b	0.44 ± 0.02	>50	>50
6b	>50	ND	ND
16a	22.3 ± 4.2	>50	>50
16b	10.0 ± 0.7	>50	>50
16c	3.9 ± 0.5	>50	>50
16d	8.9 ± 1.6	>50	>50
16e	>50	>50	>50
17	2.4 ± 0.5	>25	>50
18a	0.4 ± 0.03	>25	>25
18b	0.2 ± 0.02	>25	>25
19a	3.3 ± 1.3	5.2 ± 0.1	3.8 ± 0.3
19b	3.0 ± 0.2	5.5 ± 0.2	3.0 ± 0.4

^aActivities in recombinant Trx–TrxR insulin reduction assay.

^bCytostatic/cytotoxic effects in cellular assay. ^cND, not determined.

1, 1a strongly inhibited the activity of recombinant Trx–TrxR in the insulin reduction assay, with IC₅₀ values nearly 50-fold

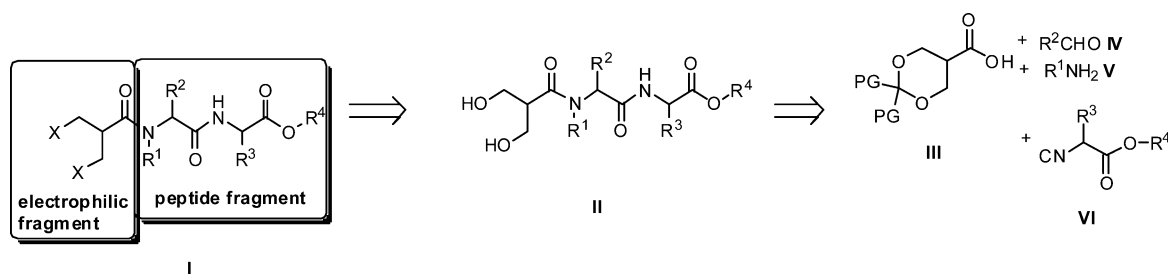


Figure 3. New concept for the synthesis of Trx–TrxR system inhibitors.

lower as compared with **3**, the Trx inhibitor currently in clinical trials. Considering that many of the Trx substrates are proteins and that peptidomimetic structures serve as efficient scaffolds for drug design,⁴⁴ we designed a target structure **I** (Figure 3), which contains an electrophilic fragment as well as a peptide mimicking backbone. The synthetic approaches, which give an access to peptidomimetics with electrophilic fragment, have not been described so far, and to the best of our knowledge, no peptidomimetic-based inhibitors of Trx–TrxR system exist. The synthesis of peptides and peptidomimetics with one or more electrophilic fragment using classical synthesis methodology is cumbersome. Also, the use of protective groups methodology is a multistep procedure, which is undesirable in searching new active structures. Therefore, the multicomponent Ugi reaction was used, which we have previously successfully employed for the synthesis of peptidomimetic scaffolds.⁴⁵ Apart from its simplicity and one-pot nature, the carboxylic group of acidic component acts as a nucleophile during Ugi reaction. Therefore, the presence of multielectrophilic centers in substrate structure is allowed.

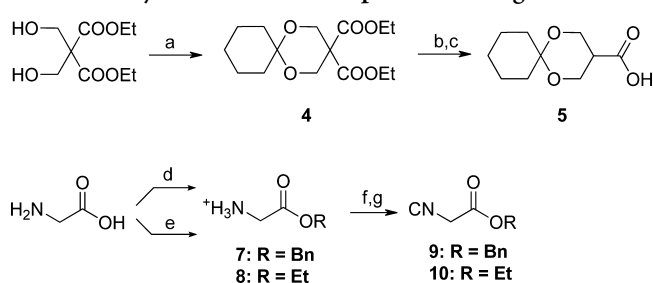
The retrosynthetic analysis and a new synthetic methodology for target compounds with a general structure **I** are presented in Figure 3. The 1,3-dihalide **I** can be obtained via functionalization of 1,3-diols **II**. An intermediate **II**, on the other hand, is a potential product of Ugi reaction with substrates **III–VI**.

2.1. Synthesis of Peptidomimetics with 1,3-Dihalogenes. For the Ugi reaction, isovaleric aldehyde, benzyl isocyanoacetate, and benzylamine were used. Isovaleric aldehyde represents a leucine residue in a product, whereas isocyanoacetate introduced glycine protected with benzyl group. Benzyl ester was used because of its easy removal, which could be useful in further functionalization. According to a retrosynthetic analysis, the introduction of the precursor of an electrophilic fragment into a peptidomimetic requires 3-hydroxy-2-hydroxymethylpropionic acid (**5**). Synthetic pathways for **5** and corresponding isocyanide are presented in Scheme 1.

Acid **5** was made from 2,2-bis(hydroxymethyl)-diethylmalonate as described before.⁴⁶ Reaction of *p*-toluenesulfonic acid and cyclohexanone with 2,2-bis(hydroxymethyl)diethylmalonate gave an acetal **4** with a 63% yield. After basic hydrolysis (50% yield) and decarboxylation in pyridine, acid **5** was obtained with 75% yield. Isocyanides **9** and **10** were obtained from their formyl derivatives using phosphorus oxychloride as a dehydrating agent as described before.⁴⁷

A further synthetic strategy of new inhibitors based on retrosynthetic analysis is presented in Scheme 2. The Ugi reaction was performed in ethanol at room temperature, and peptidomimetic **11** was obtained with a 48% yield. The next

Scheme 1. Synthesis of the Components for Ugi Reaction⁴⁸



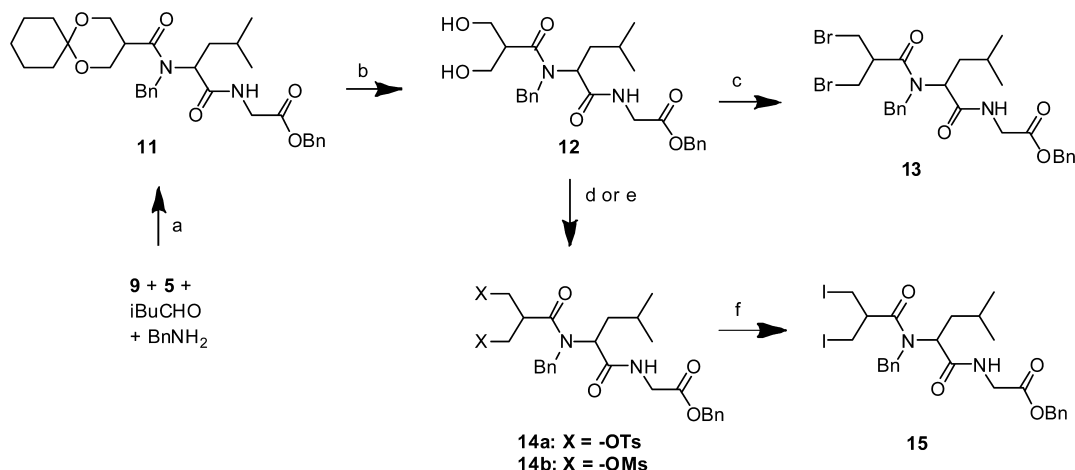
⁴⁸Reagents and conditions: (a) Cyclohexanone, *p*-TsOH, 63%. (b) KOH, EtOH, 50%. (c) Py, dioxane, 90 °C, 75%. (d) BnOH, *p*-TsCl, *p*-TsOH, 80 °C. (e) EtOH, SOCl₂, reflux, 12 h, 88%. (f) CHCOOEt, TEA, reflux, 20 h, 66–69%. (g) POCl₃, DIPEA, DCM, 0 °C, 65–85%.

step was deprotection of 1,3-diol with 80% aqueous acetic acid (compound **12**, 71% yield, Scheme 2).

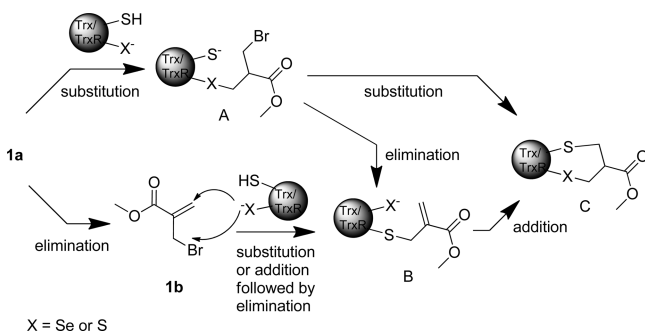
Compound **12** was a key intermediate in the synthesis of 1,3-halides as well as their analogues. Next, in the Appel reaction of **12**, the desired 1,3-dibromide **13** was obtained with 60% yield. To determine the influence of the leaving group on the Trx–TrxR system inhibition, other analogues of **13** were synthesized. Ditosylate **14a** and dimesylate **14b** were obtained with 92 and 100% yield, respectively. Then, ditosylate **14a** was chosen for substitution with sodium iodide leading to the compound **15**. The substitution was accomplished in acetone producing a compound **15** with 68% yield. This efficient synthesis provided four analogues of **1a** (**13**, **14a**, **14b**, and **15**) with peptidomimetic fragments, which were tested in the Trx–TrxR insulin reduction assay. Table 1 presents the IC₅₀ values. Surprisingly, all of the obtained analogues were inactive.

Assuming that **1a** acts through S-alkylation of selenocysteine in TrxR or cysteine residues in Trx, there are three possible mechanisms of enzyme inhibition. The first one is the alkylation of a solvent-exposed selenocysteine (or cysteine) residue via the nucleophilic substitution (Scheme 3, pathway I: **1a** → A → C). Alternatively, basic enzyme residues can promote elimination reaction of an adduct A to its α,β -unsaturated methyl methacrylate derivative B by elimination, which may be followed by the Michael addition resulting in adduct C (Scheme 3, pathway II: **1a** → A → B → C). Finally, it is also possible that **1a** may be eliminated in the assay conditions to form a more active alkylation agent methyl bromomethacrylate (**1b**), which can alkylate the cysteine (Scheme 3, pathway III: **1a** → **1b** → B → C). Considering the structures of described inhibitors, the Michael addition to a double bond might be the overall rate-determining step. It suggests that the formation of intermediate B is most likely.

To investigate this assumption, the activity of **1b** was measured, and it turned out to be more active than **1a** in the

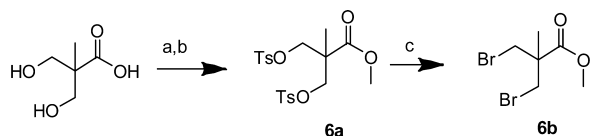
Scheme 2^a

^aReagents and conditions: (a) EtOH, 24 h, room temperature, 48%. (b) 80% AcOH, 24 h, room temperature, 71%. (c) PBr₃, PPh₃, CCl₄, 60%. (d) MsCl, TEA, DCM, 0 °C, 2 h, quant. (e) TsCl, DIPEA, DMAP cat, DCM, room temperature, 24 h, 92%. (f) NaI, acetone, reflux, 16 h, 68%.

Scheme 3. Possible Pathways of Alkylation of Cysteine Residues by 3-Bromo-2-(bromomethyl)-propionic Acid Methyl Ester^a

^aPathway I: 1a → A → C. Pathway II: 1a → A → B → C. Pathway III: 1a → 1b → B → C.

Trx–TrxR insulin reduction assay (Table 1), indicating that the proposed pathways III and II might be involved in enzyme inhibition. At this point, however, pathway I still could not be excluded. Thus, we proposed the synthesis of a model compound, which cannot undergo elimination neither to the adduct B nor to 1b during the inhibition process. Such a compound can act only via pathway I. For this purpose, the synthesis of 2-bis(bromomethyl)propionic acid methyl ester (3) was proposed employing strategy presented in Scheme 4.

Scheme 4. Synthesis of Compound 3 for Model Studies^a

^aReagent and conditions: (a) SOCl₂, methanol, reflux, 16 h, 54%. (b) *p*-TsCl, DIPEA, DMAP (cat.), DCM, 16 h, 45%. (c) LiBr, acetone, reflux, 24 h, 55%.

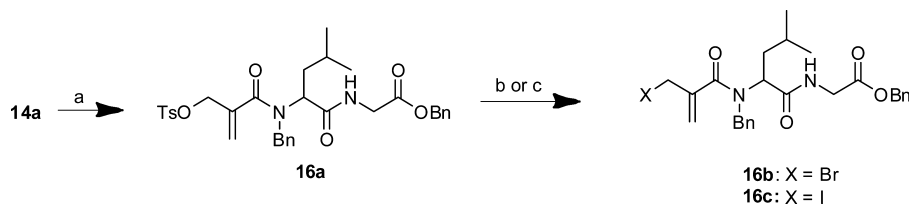
2,2-Bis(bromomethyl)propionic acid methyl ester 6b was obtained from 2,2-bis(hydroxymethyl)propionic acid, which was converted into methyl ester using thionyl chloride in

methanol (54% yield). Then, the hydroxyl groups were transformed into *p*-toluenesulphonate derivative 6a in reaction with *p*-toluenesulphonic chloride with 45% yield. Refluxing compound 6a with lithium bromide leads to the formation of a desired compound 6b with 55% yield (Scheme 4).

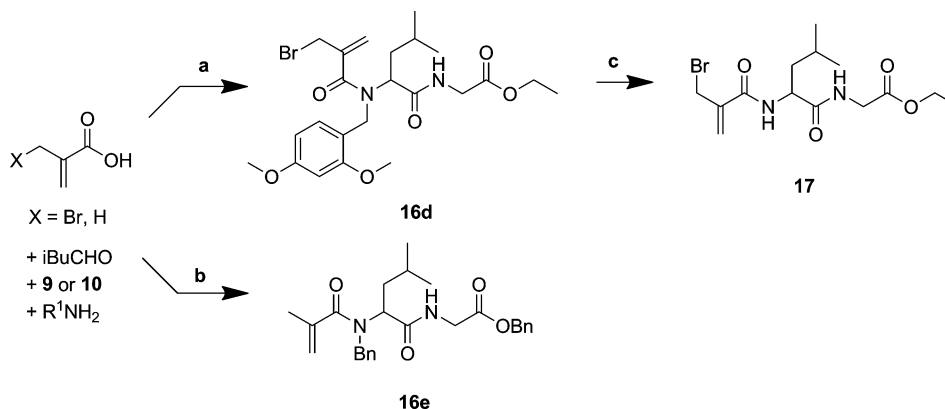
Table 1 presents the IC₅₀ values for two model compounds. In contrast to 1b, compound 6b was inactive. This lack of activity is in accordance with the mechanism presented in Scheme 3, where the elimination reaction to 1b or B is blocked. This indicates that the reaction proceeds with the α,β-unsaturated methyl methacrylate intermediate and consists of two Michael addition reactions to protein. This feature corresponds well with the structure of other known inhibitors of the Trx–TrxR system. A similar mechanism was postulated for inactivation of TrxR from *Plasmodium falciparum*.⁴¹ The interaction of organic molecules with two Michael centers with proteins was already discussed before, and acronym ETAC (equilibrium transfer alkylating cross-link reagent) was proposed.⁴⁸

2.2. Synthesis of Peptidomimetics with β-Bromoacrylamide Fragments and Their Analogues. The results presented above demonstrate that an efficient inhibitor should be able to form adduct B. Therefore, the synthesis of peptidomimetics with acrylamide fragment was designed (Scheme 5), and the influence of a leaving group in allylic position was studied. Compound 16a was obtained by elimination of tosylate from 14a in the presence of a base. Reaction with various amines such as di-isopropylethylamine (DIPEA), dimethylaminepyridin, or triethylamine (TEA) was performed; however, compound 16a was not isolated under these conditions. Finally, reaction with sodium hydride as a base leads to the product 16a with 71% yield. The substitution of the remaining tosylate resulted in compounds 16b and 16c at room temperature with yields of 95 and 93%, respectively (Scheme 5).

The inhibitory activity of compounds 16a–c was tested in the Trx–TrxR insulin reduction assay and revealed that they are relatively potent inhibitors of the Trx system, with the IC₅₀ values in the range of 3. In addition, the obtained results revealed a correlation between chemical reactivity of the electrophilic groups and their biological activity. These results

Scheme 5. Synthesis of Peptidomimetics with Acrylamide Fragments^a

^aReagents and conditions: (a) NaH, THF, $-67\text{ }^{\circ}\text{C}$ to room temperature, 2 h, 71%. (b) NaI, acetone, room temperature, 15 min, 93%. (c) LiBr, acetone, 1 h, 95%.

Scheme 6. New Synthetic Strategy for Compounds 16d, 16e, and 17^a

^aReagents and conditions: (a) $R^1 = \text{DMB}$; $X = \text{Br}$; **10**, EtOH, 6 h, $0\text{ }^{\circ}\text{C}$, 61%. (b) $R^1 = \text{Bn}$, $X = \text{H}$, **9**, EtOH, 24 h, room temperature, 36%. (c) TFA, DCM, 60 min, room temperature, 70%.

indicate that inhibition of TrxR–Trx system may be a result of covalent alkylation of cysteine or Sec residues.

Despite promising activities in enzymatic assay, compounds **16a–c** did not exert any significant cytostatic/cytotoxic activity in tumor cell lines (Table 1). This fact can be explained by high reactivity of allylic halides, which under cellular conditions may be quickly transformed into inactive derivatives. Therefore, the synthesis of less reactive **16e** was performed to study the importance of the leaving group in allylic position. An alternative synthetic pathway was employed utilizing methacrylic acid as a substrate for Ugi reaction (Scheme 6). This resulted in compound **16e** with a 36% yield.

Compounds **16a–c** contain bulky and highly hydrophobic benzyl groups, which may interfere with enzymes active site residues. Therefore, we considered compound **17**, without benzyl groups. 2,4-Dimethoxybenzylamine (DMBA) has been used before as an efficient ammonia equivalent in Ugi reactions.⁴⁵ Bromomethacrylic acid, on the other hand, has been reported to be a substrate in Ugi reaction, but the yields were poor.⁴⁹ During our studies, it turned out that acceptable yields can be achieved when the reaction is carried out at low temperatures of 0 or $-78\text{ }^{\circ}\text{C}$. After the optimization, the Ugi reaction with bromomethacrylic acid, DMBA, isovaleric aldehyde, and ethyl isocyanoacetate was performed in ethanol (Scheme 6). Compound **16d** was obtained with decent yield (61%). Then, the dimethoxybenzyl group was removed in acidic conditions using a 20% trifluoroacetic acid in dichloromethane (DCM). As a result, compound **17** was obtained with 70% yield, and its biological activity was evaluated.

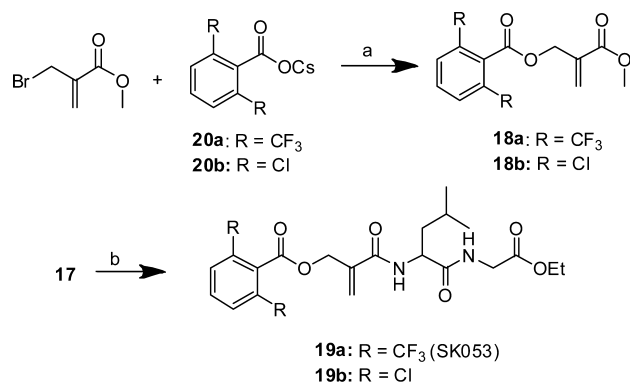
The results presented in Table 1 reveal that the activities of compounds **16b** and **17** are similar, indicating that removal of benzyl groups did not affect the activity in enzymatic assay.

Moreover, compound **16e** containing methacrylic fragment was not active, indicating that the leaving group in allylic position is indispensable for the inhibition of the Trx–TrxR system.

We turned our attention to the similar examples of biologically active compounds— α -(acyloxymethyl)ketones.⁵⁰ These compounds are efficient inhibitors of cathepsin B, a cysteine protease. The proposed mechanism of action is that carbonyl group in ketone acts as an electrophile, whereas acyloxy moiety acts as a leaving group.

Inspired by this observation, we decided to use carboxylic acid as a leaving group instead of bromine in compound **17**. Allylic esters are less reactive in substitution reaction. Therefore, we proposed a new structure of the electrophilic fragment in compounds **18a,b**. To this end, 2,6-dichlorobenzoic acid or 2,6-(trifluoromethyl)benzoic acid was used. The advantage of selected acids is the fact that the bulky 2,6-substituted acids may decrease the reactivity of the vicinal double bond, which should increase the stability and selectivity of the compound. Additionally, they are not naturally occurring compounds, so they may be more stable in the presence of endogenous esterases.

After the optimization of esterification conditions, compounds **18a,b** were obtained as model compounds from methyl bromomethacrylate (Scheme 7). Esterification of bromomethacrylate proceeds easily with appropriate cesium salts **20a,b** in acetone, resulting in compounds **18a,b** with good yields (88–97%). The compounds were tested in the Trx–TrxR insulin reduction assay. Results demonstrated that the proposed fragment was highly active, with $\text{IC}_{50} = 0.4\text{ }\mu\text{M}$ for both. Because the results with model compounds were promising, the peptidomimetics **19a,b** were synthesized. Similar conditions of

Scheme 7. Esterification of 17^a

^aReagents and conditions: (a) Acetone, reflux 4 h, 88–97%. (b) Compound 20a or 20b, acetone, reflux, 5 h, 59–87%.

substitution of 17 were employed resulting in compounds 19a and 19b with 87 and 59% yield, respectively.

The results of inhibition studies in the Trx–TrxR insulin reduction assay shown in Table 1 demonstrate that compounds 18a,b and 19a,b are promising inhibitors. However, compounds 18a and 18b are unsuitable for further development due to their chemical instability and tendency to polymerization. Our experiments revealed that these compounds do not exert cytostatic/cytotoxic effects against tumor cells even at 25 μ M concentrations (Table 1). Compound 19b exhibits significant activity in enzymatic assay; however, it is almost insoluble in biological media. Therefore, in further experiments, we focused on 19a (SK053), which is more soluble, exhibits activity in enzymatic assay, and is active against tumor cells (Table 1). The stability of 19a in phosphor-buffered saline (PBS) buffer (pH 7.4) and in pure culture medium was determined together with the reference compounds 3 and 2. Compound 19a is stable in PBS buffer but undergoes decomposition in culture medium (Figure 4). Surprisingly,

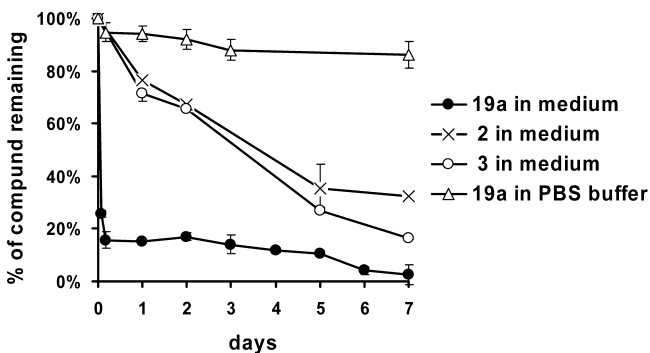


Figure 4. Stability of the investigated compounds. The kinetics of 19a degradation in 0.01 M PBS buffer (pH = 7.4) at 37 °C and the kinetics of 19a, 2, or 3 degradation in pure biological medium without serum at 37 °C (for details, see section 5.6).

19a drops to about 20% of its initial amount within 5 h and remains at this level for an additional 4 days. We have no rational explanation so far whether the activity against tumor cells results from the remaining 20% of the original compound or is rather exerted by its derivatives. Nonetheless, the inhibition of the Trx–TrxR system in the insulin reduction assay, the cytostatic/cytotoxic effects against tumor cells, and

the downstream cellular effects due to Trx–TrxR inhibition are evident (see the Results and Discussion).

In further experiments, we focused on the influence of 19a on the Trx–TrxR system in *in vitro* experiments. Mass spectrometry analysis of the recombinant human Trx incubated with 19a confirmed covalent interaction. Following incubation of the reduced form of the enzyme with 19a, we have observed additional mass peaks corresponding to Trx plus one or two inhibitor molecules attached (data not shown). Considering that human Trx molecule has five Cys residues, there seems to be some preference for certain cysteines over the others, presumably resulting from their nucleophilicity. Additional studies addressing the selectivity issue are underway. To further investigate the nature of inhibition and to determine the sensitivity of individual enzymes to 19a, we measured the Trx–TrxR system activity in two different, modified variants: (1) preincubation of Trx with 19a followed by an addition of the excess of TrxR to assess the inhibition of Trx and (2) preincubation of TrxR with 19a followed by an addition of the excess of Trx to assess the inhibition of TrxR (for details, see the Experimental Section). Interestingly, we have observed a potent, dose and time dependent inhibition of insulin reduction in both variants (Figure 5).

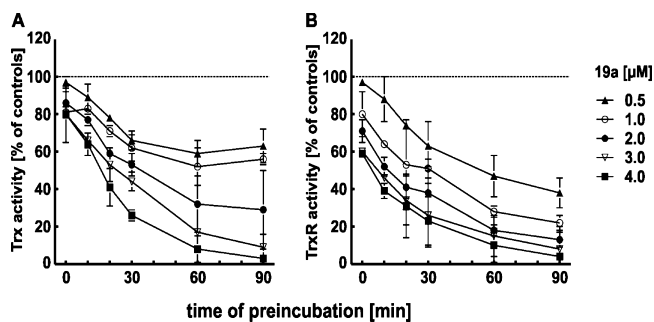


Figure 5. Time-dependent inhibition of Trx and TrxR activities. (A) Trx was first incubated with TrxR and NADPH for 20 min. Subsequently, 19a at concentrations of 2.5–20 μ M was added for preincubation before the addition of Trx substrates. To start the enzymatic reaction Trx and 19a were 5-fold diluted with insulin and additional NADPH and TrxR, and the activity was measured with the insulin reduction assay. (B) TrxR was first incubated with NADPH for 10 min and subsequently preincubated with 19a followed by addition of insulin and Trx. Compound 19a concentrations presented in the figure correspond to final inhibitor concentrations after dilution. Data points were measured in triplicate in individual experiments, and error bars represent SD.

Moreover, incubation of Raji tumor cells with 19a resulted in decreased Trx–TrxR system activity (Figure 6) and exhibited significant cytostatic/cytotoxic effects against these cells. Therefore, 19a was tested in a wider range of tumor cells with 3 used as a reference. In many cases, the cytostatic/cytotoxic effects of 19a were slightly better or very similar to those of 3 (Table 2). Experiments with normal cells (murine bone marrow cells (mBM), mouse embryonic fibroblasts (MEF), and human peripheral blood mononuclear cells (hPBMC) revealed that 19a exerts cytostatic/cytotoxic effects toward rapidly proliferating MEFs but demonstrates 5–8 times weaker activity toward nonproliferating cells as compared with tumor cells (Table 2).

To further investigate the biologic effects of Trx–TrxR system inhibitors, Raji cells were incubated with 3 or 19a, and

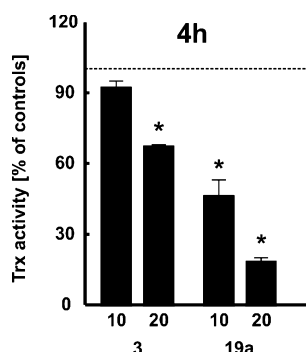


Figure 6. Incubation of tumor cells with **19a** inhibits Trx activity. Raji cells were incubated with either **3** or **19a** for 4 h. Then, tumor cells were washed three times with PBS and lysed, and the Trx activity was measured with Trx–TrxR insulin reduction assay. Data points were measured in triplicate in individual experiments ($n = 3$), and error bars represent SD; * $P < 0.05$, Student's t test.

Table 2. Cytostatic/Cytotoxic Effects of **3** and **19a** (LD_{50} , μM)

tumor cell line	3	19a
EMT6	11.6 ± 0.6	5.2 ± 0.1
PANC02	3.9 ± 0.2	3.8 ± 0.3
CT26.WT	5.2 ± 0.4	3.3 ± 0.1
B78	5.0 ± 0.3	4.3 ± 0.1
RAJI	8.8 ± 0.9	3.7 ± 0.3
Ramos	3.4 ± 0.2	3.7 ± 0.3
K562	5.5 ± 0.6	4.0 ± 0.3
T24	4.6 ± 0.6	5.6 ± 0.3
mBM ^a	>12.5	>12.5
MEF ^a	2.7 ± 0.4	2.9 ± 0.5
hPBMC ^a	>25	>25

^aNormal cells: MEF, mouse embryo fibroblasts; $n \geq 3$.

the amounts of Trx at mRNA and protein levels were measured. These studies revealed that both compounds induce expression of Trx at mRNA and protein levels (Figure 7), indicating that this might be a rescue response of cells adopting to a condition of decreased enzymatic activity of Trx.

Trx has been shown to participate in activation of various transcription factors, including NF- κ B and AP-1.^{3,4} Therefore, to investigate whether **19a** can modulate their activity HeLa cells were transiently cotransfected with p-NF κ B-luc and p-AP-1-luc as well as with Renilla reporter plasmids. A 6 h stimulation

of cells with the combination of tumor necrosis factor (TNF) and interferon (IFN)- γ resulted in activation of NF- κ B promoter activity that was inhibited by **19a** (Figure 8A). Also, ionomycin-induced AP-1 promoter activity was suppressed by **19a** (Figure 8B). Because Trx also has a weak H₂O₂ scavenging activity, the influence of **19a** on the fluorescence of CM-H₂DCFDA, a cell-permeant indicator for ROS, was measured in HeLa cells incubated with H₂O₂. The results of these experiments revealed that **19a** increases CM-H₂DCFDA fluorescence but only at the higher 10 μM concentration (Figure 8C).

Therefore, a potential antitumor activity of **19a** was evaluated in an in vivo study. For these experiments, BALB/c mice were subcutaneously inoculated with 3.5×10^5 of murine breast carcinoma (EMT6) cells and were intraperitoneally treated with two doses of **19a** dissolved in dimethylsulfoxide (DMSO) (40 and 80 mg/kg daily, for 7 consecutive days starting from day 7 after inoculation of tumor cells). Control mice received DMSO in the same treatment schedule. For the comparison of antitumor activity, another group of BALB/c mice was treated with **3** administered at dose of 14 mg/kg (equimolar to 40 mg/kg of **19a**). Unexpectedly, mice treated with **3** experienced a significant weight loss and died within 5 days of the treatment. In contrast, administration of **19a** was well tolerated by all animals (no significant weight loss and no mortality). Importantly, in mice treated with 80 mg/kg of **19a**, a statistically significant retardation of tumor growth and prolongation of the survival time was observed (Figure 9).

3. CONCLUSIONS

The Trx–TrxR system is a promising molecular target for antitumor compounds. The literature study on potential mechanisms of action of known inhibitors of this system allowed us to design novel, potent compounds reactive with the nucleophilic residues within the active sites of Trx and TrxR. The new and relatively simple synthetic approach employing the Ugi reaction with reactive bromomethacrylic acid as a substrate allowed the synthesis of peptidomimetics with various electrophilic fragments that were analogues of the known Trx system inhibitor **1**. During this study, various electrophilic fragments in target compounds were tested as potential Trx system inhibitors, and their cytostatic/cytotoxic activity against tumor cells was measured. As a result, a simple, three-step synthesis is described, which results in a new class of a wide spectrum of β -acyloxyacrylamides. This new class, represented

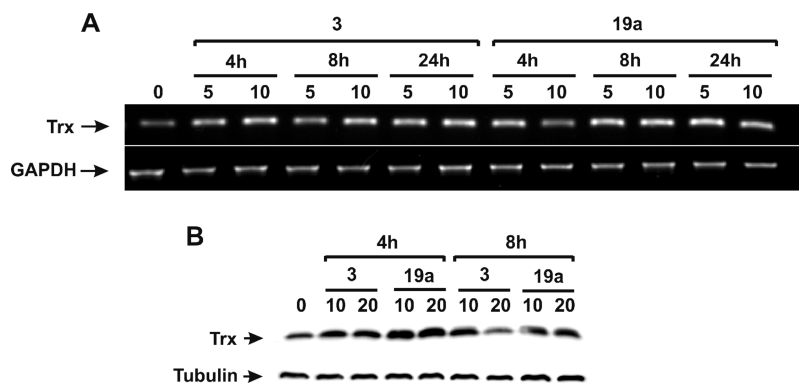


Figure 7. Expression of Trx in tumor cells incubated with **3** or **19a**. Following incubation of Raji cells with **3** or **19a**, the levels of mRNA (A) or protein (B) for Trx were measured in tumor cell lysates.

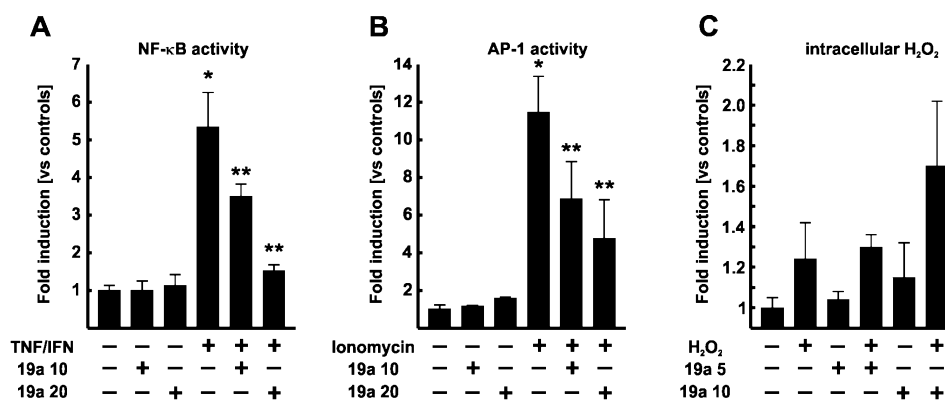


Figure 8. Compound 19a modulates Trx target activities. Data points were measured in triplicate in individual experiments ($n = 3$), and error bars represent SD; * $P < 0.05$ vs controls, ** $P < 0.05$ vs TNF/IFN, or ionomycin group; Student's t test.

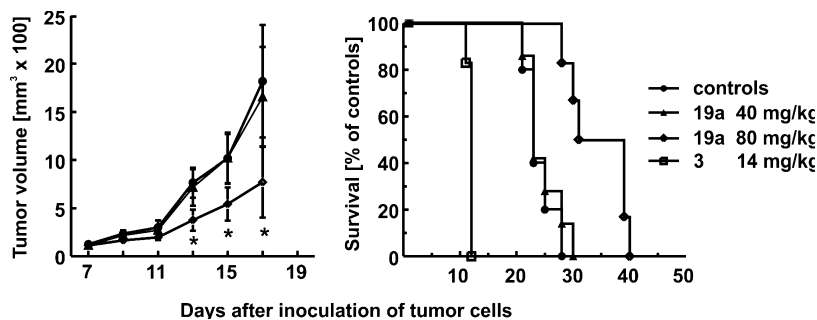


Figure 9. Antitumor effects of Trx inhibitors. Balb/c mice were inoculated with 3.5×10^5 of EMT6 cells. Tumor treatment started on day 7 after inoculation of tumor cells. Compound 19a or 3 was administered daily ip for 7 consecutive days (administration of 3 was terminated after three doses due to a significant weight loss death of the first animal). Control mice received DMSO. Graphs show the influence of the treatment on the growth of tumors and survival of mice. * $P < 0.05$ (two way Student's t test) in comparison with all other groups.

by 19a, turned out to effectively inhibit the Trx–TrxR system activity and to exert potent antiproliferative and/or cytotoxic effects against tumor cells in in vitro studies as well as significant antitumor activity in an in vivo tumor model. It is noteworthy that cytotoxicity of 19a toward various tumor cell lines correlates with the in vitro Trx–TrxR inhibition potency (LD_{50} between 2.9 and 5.6 μM vs 3.3 μM IC_{50}). Moreover, 19a turned out to be less toxic in mice as compared with 3. The exact mechanism of action of this inhibitor has not been established; however, it will be the subject of our further studies. The structure of 19a will be also further optimized, especially in terms of its peptidomimetic fragment. Furthermore, we cannot exclude that the inhibition of targets other than Trx–TrxR system can contribute to antitumor activity of the presented compounds.

4. EXPERIMENTAL SECTION

4.1. General. NMR spectra were measured with Varian 200 Gemini, Varian 400 Gemini, and Bruker AM 500 spectrometers, with TMS used as an internal standard. TLCs were performed with silica gel 60 (230–400 mesh or 70–230 mesh, Merck) and silica gel 60 PF254 (Merck). CHN analysis was performed on a Vario EL III (Elementor) elemental analyzer. High-resolution mass spectrometry (HR-MS) spectra were recorded on an Mariner (PerSeptive Biosystems) apparatus. Methyl bromomethyl acrylate (1b), methyl methacrylate (MMA), and all starting materials were purchased in Sigma-Aldrich. HPLC experiments were carried out on a Kromasil C-18 column, $\lambda = 230$ nm: method 1 [eluent: acetonitrile/water 55:45 (v/v), flow of 1 mL/min]; method 2 [eluent: acetonitrile/water 45:55 (v/v), flow of 0.8 mL/min]; and method 3 [eluent: acetonitrile/water 3:2 (v/v), flow of 1.0 mL/min]. Compound 3 synthesis was performed

as described before (NMR spectra was the same as described, and the purity was confirmed by HPLC as well as elemental analysis).⁵¹ All key compounds were proven by HPLC method to show >95% purity.

4.2. Synthesis of Peptidomimetics. **4.2.1. Synthesis of {2-[Benzyl-(3-bromo-2-bromomethyl-propionyl)amino]-4-methylpentanoylamino}acetic Acid Benzyl Ester (13).** Compound 12 (100 mg, 0.2 mmol) was dissolved in DCM (10 mL), and carbon tetrachloride (148 mg, 0.4 mmol) and triphenylphosphine (123 mg, 0.5 mmol) were added. The mixture was stirred for 24 h. The solvent was evaporated, and the residue was purified by flash chromatography (silica gel, $R_f = 0.82$, hexane:ethyl acetate, 5:5, v/v). A colorless oil was obtained (76 mg, 60% yield). ¹H NMR (200 MHz, CDCl₃): δ 0.77 (d, $J = 6.4$ Hz, 3H, CHCH₃), 0.85 (d, $J = 6.4$ Hz, 2H, CHCH₃), 1.20–1.62 (m, 2H, CH₂CH(CH₃)₂), 1.64–1.88 (m, 1H, CH(CH₃)₂), 3.21–3.88 (m, 1H, CHCH₂), 4.00–4.78 (m, 3H, ArCH₂, CHCO), 4.97–5.30 (m, 3H, ArCH₂, NH), 7.08–7.40 (m, 10H, ArH). ¹³C NMR (50 MHz, CDCl₃): δ 22.7, 23.1, 25.6, 30.0, 36.6, 41.4, 48.1, 56.0, 64.5, 68.0, 126.5, 126.9, 127.8, 128.2, 128.8, 129.0, 169.5, 171.3, 173.2. HR-MS (ESI, [M + Na⁺]) calcd for C₂₆H₃₂N₂O₄Br₂Na, 617.0621; found, 617.0643.

4.2.2. Synthesis of (2-{Benzyl-[3-(toluene-4-sulfonyloxy)-2-(toluene-4-sulfonyloxymethyl)propionyl]amino}-4-methylpentanoylamino)acetic Acid Benzyl Ester (14a). To a solution of 12 (30 mg, 0.06 mmol) in DCM (2 mL) *N,N*-diethylaminepyridine (10 mg) and *N,N*-diisopropyl-*N*-ethylamine (0.027 mL, 2.5 mmol) were added. The solution of *p*-toluenesulfonylchloride (27 mg, 0.14 mmol) in DCM (3 mL) was then added. The reaction was carried out at room temperature for 18 h. The solvent was evaporated, and the residue was purified by flash chromatography (silica gel, $R_f = 0.69$, 5:5, hexane:ethyl acetate, v/v). A 45.6 mg amount of colorless oil was obtained (92% yield). ¹H NMR (200 MHz, CDCl₃): δ 0.85 (d, $J = 6.4$ Hz, 3H, CHCH₃), 0.93 (d, $J = 6.2$ Hz, 3H, CHCH₃), 1.35–1.63 (m, 2H, CH₂CH(CH₃)₂), 1.76 (s, 1H, CH(CH₃)₂), 2.50 (s, 3H, ArCH₃), 2.53 (s, 3H, ArCH₃), 3.32–3.6 (m, 1H, CHCO), 4.03–4.27 (m, 6H,

OCH₂, ArCH₂N), 4.53–4.76 (m, 2H, CH₂CO), 5.24 (s, 2H, ArCH₂O), 6.75–6.80 (m, 1H, NH), 7.16–7.42 (m, 14H, ArH), 7.70–7.83 (m, 4H, ArH). ¹³C NMR (50 MHz, CDCl₃): δ 20.0, 22.8, 25.4, 37.0, 41.6, 42.8, 48.8, 56.6, 67.3, 67.9, 68.2, 126.4, 128.0, 128.2, 128.6, 128.7, 128.9, 129.2, 130.3, 130.4, 132.4, 136.9, 145.5, 169.9, 170.8, 171.3. Anal. calcd for C₄₀H₄₆N₂O₁₀S₂: C, 61.68; H, 5.95; N, 3.60; S, 8.23. Found: C, 61.76; H, 5.81; N, 3.55; S, 8.46%.

4.2.3. Synthesis of {2-[Benzyl-(3-methanesulfonyloxy-2-methanesulfonyloxymethyl-propionyl)amino]-4-methyl-pentanoylamino}acetic Acid Benzyl Ester (14b). Compound **12** (35 mg, 0.07 mmol) was dissolved in anhydrous DCM (3 mL), and TEA (25 μL, 0.18 mmol) was added. The mixture was cooled to 0 °C. Methylsulfonyl chloride (15 μL, 0.17 mmol) was added dropwise. The reaction was allowed to reach room temperature and was stirred for 24 h. The solvent was evaporated, and the residue was filtered through silica gel giving 37 mg of colorless oil (quant. yield). ¹H NMR (200 MHz, CDCl₃): δ 0.80 (t, J = 6.8 Hz, 6H, CHCH₃), 1.25–1.58 (m, 2H, CH₂CH(CH₃)₂), 1.64–2.05 (m, 1H, CH(CH₃)₂), 3.02–3.18 (m, 7H, SCH₃, CHCO), 3.72–3.92 (m, 1H, CHCO), 4.00–4.34 (m, 4H, OCH₂), 4.61 (s, 2H, ArCH₂N), 5.16 (s, 2H, ArCH₂O), 7.10–7.17 (m, 2H, ArH), 7.23–7.38 (m, 8H, ArH). ¹³C NMR (50 MHz, CDCl₃): δ 22.6, 22.7, 22.8, 23.1, 25.5, 26.0, 27.7, 36.9, 38.3, 40.4, 41.4, 48.5, 55.9, 61.3, 61.6, 67.5, 98.4, 126.1, 127.9, 128.8, 128.9, 129.0, 129.2, 135.5, 137.4, 169.7, 171.3, 173.8. HR-MS (ESI, [M + Na⁺]) calcd for C₂₈H₃₈N₂O₁₀S₂Na, 649.1860; found, 649.1870.

4.2.4. Synthesis of {2-[Benzyl-(3-iodo-2-iodomethyl-propionyl)-amino]-4-methyl-pentanoylamino}acetic Acid Benzyl Ester (15). To a solution of **14a** (46.4 mg, 0.06 mmol) in acetone (3 mL), sodium iodide was added (54.5 mg, 0.36 mmol). The mixture was refluxed for 24 h. The solvent was evaporated, and the residue was purified by flush chromatography (silica gel, R_f = 0.87, 7:3, hexane:ethyl acetate, v/v). The product was obtained as colorless oil (27.8 mg, 68% yield). ¹H NMR (200 MHz, CDCl₃): δ 0.85–0.90 (m, 6H, CH(CH₃)₂), 1.46–1.70 (m, 2H, CH₂CH(CH₃)₂), 1.86–1.96 (m, CHCH₃, 1H), 3.18–3.23 (m, 5H, ICH₂, CHCO), 4.01–4.05 (m, 2H, NCH₂Ar), 4.66 (d, J = 6.4 Hz, 2H, NCH₂CO), 5.18 (s, 2H, ArCH₂O), 7.24–7.37 (m, 10H, ArH). ¹³C NMR (50 MHz, CDCl₃): δ 5.2, 5.6, 22.8, 23.1, 23.1, 25.5, 37.4, 41.6, 48.2, 49.4, 56.8, 67.5, 126.9, 128.2, 128.7, 128.9, 129.0, 129.4, 135.5, 137.1, 169.6, 170.9, 173.6. Anal. calcd for C₂₆H₃₂I₂N₂O₄: C, 45.24; H, 4.67; N, 4.06. Found: C, 45.34; H, 4.77; N, 4.05.

4.2.5. Synthesis of {2-[Benzyl-[2-(toluene-4-sulfonyloxymethyl)-acryloyl]-amino]-4-methyl-pentanoylamino}acetic Acid Benzyl Ester (16a). The solution of compound **14a** (27 mg, 0.4 mmol) in tetrahydrofuran (THF) was cooled to –67 °C under atmosphere of nitrogen. Sodium hydride (1 mg, 0.4 mmol) was added. The mixture was allowed to stand to room temperature and stirred for 1 h. The solvent was evaporated, and the residue was purified by flush chromatography (silica gel, R_f = 0.59, 5:5, hexane:ethyl acetate, v/v). The product was obtained as a colorless oil (15 mg, 71% yield). ¹H NMR (200 MHz, CDCl₃): δ 0.77–0.85 (m, 6H, CHCH₃), 1.40–1.68 (m, 1H, CHCH₃), 1.80–2.10 (m, 2H, CH₂CHCH₃), 2.44 (s, 3H, ArCH₃), 3.92 (d, J = 5.8 Hz, 2H, OCH₂), 3.80–4.0 (m, 5H, ArCH₂N, NCH₂CO, NCHCO), 5.17 (s, 2H, ArCH₂O), 5.44 (s, 1H, CH=C), 5.55 (s, 1H, CH=C), 7.23–7.34 (m, 12H, ArH), 7.77 (d, J = 8.6 Hz, 2H, ArH). ¹³C NMR (50 MHz, CDCl₃): δ 22.0, 22.9, 23.8, 25.3, 32.7, 41.6, 67.4, 69.1, 103.4, 119.9, 127.9, 128.1, 128.4, 128.6, 128.7, 128.9, 130.3, 135.6, 137.9, 169.8, 170.7, 171.3. Anal. calcd for C₂₇H₃₆N₂O₆ + 0.5H₂O: C, 64.37; H, 6.38; N, 4.55; S, 5.21. Found: C, 64.31; H, 6.33; N, 4.41; S, 5.17.

4.2.6. Synthesis of {2-[Benzyl-(2-bromomethyl-acryloyl)amino]-4-methyl-pentanoylamino}acetic Acid Benzyl Ester (16b). To a solution of compound **16a** (90 mg, 0.1 mmol) in acetone (3 mL) lithium bromide was added (12 mg, 0.14 mmol). The mixture was stirred for 1 h at room temperature. The solvent was evaporated, and the residue was purified by flush chromatography (silica gel, R_f = 0.26, 7:3, hexane:ethyl acetate, v/v). The product was obtained as oil (80 mg, 95% yield). ¹H NMR (500 MHz, CDCl₃): δ 0.82–0.87 (m, 6H, CH(CH₃)₂), 1.56–1.82 (m, 2H, CH₂CH(CH₃)₂), 1.96–2.01 (m, 1H, CH₂CH(CH₃)₂), 3.95 (m, 2H, BrCH₂), 4.20–4.25 (m, 2H, ArCH₂N), 4.60–4.81 (m, 3H, NCHCO, NCH₂CO), 5.18 (s, 2H, ArCH₂O), 5.37

(s, 1H, HC=C), 5.49 (s, 1H, HC=C), 7.32–7.37 (m, ArH 10H). ¹³C NMR (125 MHz, CDCl₃): δ 22.4, 23.0, 25.1, 26.9, 33.2, 37.3, 41.3, 41.5, 52.4, 67.1, 118.9, 127.5, 128.4, 128.5, 128.6, 135.2, 140.1, 169.9, 170.4, 171.9. Anal. calcd for C₂₆H₃₁BrN₂O₄: C, 60.59; H, 6.06; N, 5.43. Found: C, 60.92; H, 6.11; N, 5.01. HR-MS (ESI, [M + Na⁺]) calcd for C₂₆H₃₁N₂O₄BrNa, 537.1359; found, 537.1356.

4.2.7. Synthesis of {2-[Benzyl-(2-iodomethyl-acryloyl)amino]-4-methyl-pentanoylamino}acetic Acid Benzyl Ester (16c). To a solution of compound **16a** (15 mg, 0.02 mmol) in acetone (1 mL), sodium iodide was added (22.6 mg, 0.15 mmol). The mixture was stirred for 1 h in room temperature. The solvent was evaporated, and the residue was purified by flush chromatography (silica gel, R_f = 0.58, 7:3, hexane:ethyl acetate, v/v). A colorless oil was obtained. (8 mg, 93%). ¹H NMR (400 MHz, CDCl₃): δ 0.76–0.88 (m, 6H, CH(CH₃)₂), 1.40–1.80 (m, 2H, CH₂CH(CH₃)₂), 1.82–2.04 (m, 1H, CH₂CH(CH₃)₂), 3.95 (s, 2H, ICH₂), 4.12 (s, 2H, ArCH₂N), 4.50–4.80 (m, 3H, NCHCO, NCH₂CO), 5.18 (s, 2H, ArCH₂O), 5.28 (s, 1H, HC=C), 5.48 (s, 1H, HC=C), 7.26–7.36 (m, 10H, ArH). ¹³C NMR (100 MHz, CDCl₃): δ 5.75, 22.6, 23.1, 25.6, 41.7, 67.4, 118.1, 127.8, 128.7, 128.8, 128.9, 141.3, 169.6, 170.2, 171.3. Anal. calcd for C₂₆H₃₁I₂N₂O₄ + H₂O: C, 53.80; H, 5.73; N, 4.83. Found: C, 53.87; H, 5.73; N, 4.65. HR-MS (ESI, [M + Na⁺]) calcd for C₂₆H₃₁N₂O₄I Na, 585.1221; found, 585.1233.

4.2.8. Synthesis of {2-(2-Bromomethyl-acryloylamino)-4-methyl-pentanoylamino}acetic Acid Ethyl Ester (17). Compound **16d** (117 mg, 0.23 mmol) dissolved in DCM (2 mL) and trifluoroacetic acid (475 μL) was added. The mixture was stirred for 1 h at room temperature. DCM was added (4 mL). A saturated solution of sodium bicarbonate was added until the mixture become transparent. The water phase was extracted with DCM (3 × 8 mL). The combined organic layer was washed with brine, dried over anhydrous magnesium sulfate, and filtered, and volatiles were evaporated. The residue was purified by flush chromatography (silica gel, R_f = 0.25, 6:4, hexane:ethyl acetate, v/v). A 58 mg amount of white solid (mp = 78–79 °C) was obtained (70% yield). ¹H NMR (200 MHz, CDCl₃): δ 0.87–0.94 (m, 6H, CH(CH₃)₂), 1.25 (t, J = 7.2 Hz, 3H, OCH₂CH₃), 1.38–1.70 (m, 3H, CH₂CH(CH₃)₂), 3.88–4.12 (m, 2H, NHCH₂), 4.12–4.22 (m, 4H, OCH₂CH₃; BrCH₂C), 4.60–4.78 (m, 1H, NHCH), 5.69 (s, 1H, CCHH), 5.85 (s, 1H, CCHH), 6.90 (d, J = 8.0 Hz, 1H, NH), 7.14 (m, 1H, NH). ¹³C NMR (50 MHz, CDCl₃): δ 14.5, 22.4, 23.3, 25.1, 30.7, 41.4, 41.7, 52.1, 61.8, 123.0, 141.3, 166.4, 170.0, 172.6. HR-MS (ESI, [M + Na⁺]) calcd for C₁₄H₂₃BrN₂O₄ Na, 385.0733; found, 385.0740.

4.3. General Procedure II for Synthesis Compounds 19a,b.

Compound **17** (1 mmol) was dissolved in acetone. The carboxylic acid cesium salt (5 mmol) was suspended in the mixture. The reaction was refluxed for 4 h. The solvent was evaporated, and the residue was suspended in ethyl acetate. The organic layer was washed with water and brine and dried with magnesium sulfate. The solvent was evaporated, and the residue was purified using flush chromatography.

4.3.1. Synthesis of 2,6-Bis-trifluoromethyl-benzoic Acid 2-[1-(Ethoxycarbonylmethyl-carbamoyl)-3-methyl-butylcarbamoyl]allyl Ester (19a). General Procedure II. Yield, 87%; white solid; mp = 114–115 °C; R_f = 0.61 (1:1, hexane:ethyl acetate, v/v). ¹H NMR (200 MHz, CDCl₃): δ 0.85–0.91 (m, 6H, CH(CH₃)₂), 1.24 (t, J = 7.2 Hz, 3H, OCH₂CH₃), 1.51–1.70 (m, 3H, CH₂CH(CH₃)₂), 3.84–4.08 (m, 2H, NHCH₂COO), 4.17 (q, J = 7.2 Hz, 2H, OCH₂CH₃), 4.51–4.67 (m, 1H, NCH), 5.10 (s, 2H, OCH₂C), 5.79 (s, 1H, CCHH), 6.02 (s, 1H, CCHH), 6.74 (d, J = 8.2 Hz, 1H, NH), 6.98–7.03 (m, 1H, NH), 7.72 (m, 1H, ArH), 7.91 (d, J = 7.8 Hz, 2H, ArH). ¹³C NMR (50 MHz, CDCl₃): δ 14.4, 22.4, 23.0, 25.0, 30.7, 41.2, 41.6, 51.9, 61.8, 65.6, 120.0, 124.3, 125.8, 129.0, 129.7, 130.2, 130.7, 137.9, 164.8, 166.4, 169.9, 172.6. Anal. calcd for C₂₃H₂₆F₆N₂O₆: C, 51.11; H, 4.85; N, 5.18. Found: C, 51.00; H, 5.07; N, 4.86.

4.3.2. Synthesis of 2,6-Dichloro-benzoic Acid 2-[1-(Ethoxycarbonylmethyl-carbamoyl)-3-methyl-butylcarbamoyl]allyl Ester (19b). General Procedure II. Yield, 59%; white solid; mp = 120–121 °C, R_f = 0.34 (1:1, hexane:ethyl acetate, v/v). ¹H NMR (200 MHz, CDCl₃): δ 0.83 (d, J = 6 Hz, 6H, CH(CH₃)₂), 1.20 (t, J = 7.0 Hz, 3H, OCH₂CH₃), 1.47–1.69 (m, 3H, CH₂CH(CH₃)₂), 3.81–4.07 (m, 2H,

NHCH₂COO), 4.12 (q, *J* = 7.0 Hz, 2H, OCH₂CH₃), 4.51–4.60 (m, 1H, NCH), 5.07 (d, *J* = 4.2 Hz, 2H, OCH₂C), 5.78 (s, 1H, CCHH), 6.00 (s, 1H, CCHH), 6.56 (d, *J* = 8.2 Hz, 1H, NH), 6.77 (bs, 1H, NH), 7.20–7.25 (m, 3H, ArH). ¹³C NMR (50 MHz, CDCl₃): δ 14.5, 22.4, 23.2, 25.1, 41.2, 41.7, 51.9, 61.9, 65.1, 124.6, 128.2, 131.4, 132.2, 138.1, 166.4, 169.8, 172.28. HR-MS (ESI, [M + Na⁺]) calcd for C₂₁H₂₆Cl₂N₂O₆ Na, 495.1060; found, 495.1081.

4.4. Cloning, Expression, and Purification of Recombinant Human Trx. The gene-encoding human Trx-1 was amplified by PCR on the cDNA obtained from human embryonic kidney cell line HEK-293T and cloned into pET15-mod, a derivative of Novagen pET15b(+) vector, containing six additional N-terminal histidine codons.⁵² The fusion protein overexpression was performed in *Escherichia coli*, strain BL21 Codon Plus RIL. Bacterial cells were grown at 37 °C until they reached an OD₆₀₀ = 0.7–0.9 and then after induction with 0.5 mM isopropyl β-D-1-thiogalactopyranoside (IPTG), shifted to 30 °C for additional 16 h. For purification, cells were disrupted in lysozyme-containing buffer by sonication and ultracentrifuged, and the soluble fraction was subjected to nickel affinity chromatography and subsequently to gel filtration chromatography (column Superdex 75 High Load 16/60, Amersham Pharmacia) in reducing conditions [buffer: 10 mM Tris, pH 7.5, 100 mM NaCl, and 10 mM dithiothreitol (DTT)]. Pure protein was concentrated with Vivaspin concentrator (10 kDa cutoff) to the concentration about 20 mg/mL and frozen at –20 °C after the addition of glycerol for cryoprotection. Before use, Trx was dialyzed two times against 10 mM Tris, pH 7.5, buffer to remove DTT, glycerol, and NaCl.

4.5. Cell Lines and Reagents. Murine mammary carcinoma (EMT6), murine colon carcinoma (CT26.WT), human bladder carcinoma (T24), and human Burkitt's lymphoma (Ramos, Raji) cell lines were purchased from ATCC (Manassas, VA). The B78-H1 melanoma (herein named B78), a poorly immunogenic amelanotic subclone of murine B16 melanoma cell line, was kindly provided by Dr. Lloyd H. Graf (University of Chicago, Chicago, IL). Murine pancreatic carcinoma cells (Panc 02) were kindly obtained from Carsten Ziske (Rheinische Friedrich-Wilhelms-Universität, Bonn, Germany). The human erythromyeloblastoid leukemia cell line (K562) was purchased from DSMZ (Braunschweig, Germany). Cells were cultured in RPMI-1640 (CT26.WT, Ramos, Raji, K562), Dulbecco's modified Eagle's medium (EMT6, B78, Panc02) or McCoy's medium (T24) supplemented with 10% heat-inactivated fetal bovine serum (Invitrogen, Carlsbad, CA) and antibiotic/antimycotic solution (Sigma, St. Louis, MO). mBM cells were collected from Balb/c female mice and cultured in ISCOV medium (Invitrogen) supplemented with 10% heat-inactivated fetal bovine serum (Invitrogen), antibiotic/antimycotic solution (Sigma), and 100 U of IL-3 (Peprotech, NJ). Histopaque 1077 was used to isolate hPBMC from healthy donors. After a 30 min centrifugation (700g, 25 °C), white blood cell rings were washed twice with PBS and resuspended in RPMI. MEFs were isolated from Balb/c mouse fetuses on embryonic day 13.5 (E 13.5) by trypsin (0.2%) digestion at 37 °C for 10 min in PBS. MEFs were cultured in Dulbecco's modified Eagle's medium. All synthesized compounds were dissolved in DMSO to produce stock solution of 10 mM.

4.5.1. Cytostatic/Cytotoxic Assays. The cytostatic/cytotoxic effects were measured using crystal violet staining (EMT6, CT26.WT, T24, B78, and Panc 02) or 3-[4,5-dimethylthiazol-2-yl]-2,5-diphenyltetrazolium bromide (MTT) assay (Raji, Ramos, and K562), or 2,3-Bis(2-methoxy-4-nitro-5-sulfophenyl)-2H-tetrazolium-5-carbox-anilide (XTT) assay (hPBMC, mBM). First, tumor cells were dispensed into 96-well plates (Sarstedt, Numbrecht, Germany). The following day, the investigated compounds were added at indicated concentrations for a 72 h incubation. Then, the adherent cells were rinsed with PBS and stained with 0.5% crystal violet in 2% ethanol for 10 min at room temperature. Next, plates were washed with tap water, and cells were lysed with 2% SDS solution. The absorbance was measured at 595 nm using an ELISA reader (SLT Labinstrument GmbH, Salzburg, Austria). To evaluate cytostatic/cytotoxic effects in nonadherent cells, after a 72 h of incubation with **19a** or **3**, MTT solution in a concentration of 5 mg/mL was added to each well of plate. After

subsequent 4 h, plates were centrifuged, and cells were lysed with DMSO. Finally, the absorbance was measured at 570 nm. The XTT assay was used to evaluate the cytostatic/cytotoxic effects in hPBMC and mBM. After a 4 h incubation with XTT (0.3 mg/mL), the absorbance was measured at 490 nm with the reference wavelength of 690 nm. The relative viability of cells (% of control cultures incubated with medium and corresponding concentrations of inhibitors solvent – DMSO, never exceeding 1%) was calculated as follows: relative viability = [(A_e – A_b)/(A_c – A_b)] × 100, where A_b is the background absorbance, A_e is the experimental absorbance, and A_c is the absorbance of untreated controls.

4.5.2. Trx/TrxR Insulin Reduction Assays. To measure the activity of investigated compounds, the Trx–TrxR insulin reduction kit (IMCO Co., Stockholm, Sweden) was used. The procedure is based on the reduction of insulin by Trx.⁴³ The reduced form of Trx is maintained with TrxR and NADPH. The activity was measured in a final volume of 50 μL containing 50 mM Tris-HCl buffer (pH 7.6), 20 mM EDTA, 0.8 μM NADPH, 0.325 μM TrxR, 0.25 μM Trx, and 316 μM bovine insulin (Sigma Aldrich) and the indicated concentrations of studied compounds. At least seven different concentrations of studied compounds were used in individual experiments. After 30 min of incubation at 37 °C, the reaction was terminated by the addition of 8 mM DTNB [5,5'-dithiobis-(2-nitrobenzoic acid)] solution in 8 M guanidine HCl (Sigma Aldrich), to determine the number of free thiols from reduced insulin. The relative amount of yellow product thionitrobenzoate was evaluated by absorbance measurement at 412 nm. The IC₅₀ values were evaluated with Four Parameter Logistic Standard Curves Analysis using a SigmaPlot software. Data points were measured in triplicates in individual experiments, and IC₅₀ values are EC₅₀ ± SD, *n* ≥ 3. To measure the Trx activity in cells, Raji tumor cells were incubated with **3** or **19a** for 4 h, washed three times with PBS, and lysed in 0.1% NP40 buffer, supplemented with Complete protease inhibitors cocktail (Roche Diagnostics). The protein concentration was measured using BCA protein assay (BioRad, United Kingdom). The Trx activity was evaluated in 10 μg of total protein as described above. The reaction was performed for 20 min in 37 at 37 °C according to kit protocol (IMCO Co.).

4.5.3. Time-Dependent Inhibition of Trx and TrxR Activity. To determine the nature of inhibition of individual enzymes in the Trx–TrxR system by **19a**, two modified variants of insulin reduction assay were employed. Because of large enzyme amounts needed, we used human recombinant Trx produced according to the procedure described above (section 4.4). To assess predominantly Trx inhibition, Trx was incubated with TrxR and NADPH for 20 min to obtain reduced enzyme form and subsequently preincubated with **19a** at concentrations from 2.5 to 20 μM for 0, 10, 20, 30, 60, and 90 min at 37 °C. To start the insulin reduction, Trx and **19a** were 5-fold diluted with insulin, additional NADPH, and TrxR. The final concentrations of reaction components were as follows: 0.25 μM Trx, 6.5 μM TrxR, 1 μM NADPH, and 0.5–4 μM **19a**. To evaluate predominantly the TrxR inhibition, the enzyme was incubated with NADPH for 10 min and subsequently preincubated with **19a** at concentrations from 2.5 to 20 μM for 0, 10, 20, 30, 60, and 90 min at 37 °C. The reaction of insulin reduction was initiated by the addition of insulin and Trx. The final concentrations were as follows: 3.25 nM TrxR, 10 μM Trx, 1 μM NADPH, and 0.5–4 μM **19a**. In all experiments, the reactions of insulin reduction were performed for 30 min, at 37 °C, in Tris-HCl EDTA buffer, pH 7.6, in a final volume of 100 μL. Reactions were terminated by the addition of 8 mM DTNB solution in 8 M guanidine HCl. The relative amount of yellow product thionitrobenzoate was evaluated by absorbance measurement at 412 nm.

4.5.4. RT-PCR. RNA from Raji cells was isolated using a trizol reagent (Invitrogen) after incubation with **3** or **19a**. RT-PCR was performed with AMV reverse transcriptase (Eurex, Poland) according to manufacturer's protocol. Subsequently, PCR was done using ColorOptiTaQ DNA Polymerase (Eurex, Poland) using the following pairs of primers amplifying human Trx1: 5'-GCCAAGATGGTGAAG-CAGAT-3' (forward) and 5'-TTGGCTCCAGAAAATTCAACC-3' (reverse); and human GAPDH: 5'-CCCTTCATTGACCTCAACTA-

CATGG-3' (forward) and 5'-CCTGCTTACCACCTTCTT-GATGTC-3' (reverse).

4.5.5. Western Blotting. For Western blotting analysis, cells were cultured with **19a** and **3** for 4 and 8 h. After they were washed with PBS, the cells were lysed in 0.1% NP40 buffer supplemented with Complete protease inhibitors cocktail (Roche Diagnostics, Mannheim, Germany). The protein concentration was measured using BCA protein assay (Biorad). Equal amounts of proteins were separated on 15% SDS-polyacrylamide gel, transferred onto Protran nitrocellulose membranes (Schleicher and Schuell BioScience Inc., Keene, NH), and blocked with TBST [Tris-buffered saline (pH 7.4) and 0.05% Tween 20] with 5% BSA (Sigma Aldrich). The following antibodies were used for the overnight incubation: antithioredoxin (rabbit monoclonal, Cell Signaling) and antitubulin (mouse monoclonal, Sigma Aldrich). After extensive washing with TBST, the membranes were incubated for 45 min in corresponding HRP-coupled secondary antibodies (Jackson Immuno Research, West Grove, PA). The reaction was developed using 0.2 mM cumaric acid (Sigma Aldrich) and 1.25 mM luminol (Sigma Aldrich), diluted in 50 mM Tris-HCL (pH 7.8) and supplemented with H₂O₂, and the luminescence was acquired using Stella bioimager (Raytest, Germany).

4.5.6. Luciferase Reporter Assay. Luciferase reporter plasmids pTA-NFκB-luc and pTA-AP-1-luc were purchased from Clontech. Renilla control plasmid with a constitutive CMV promoter (pRL-CMV-luc) was purchased from Promega. Transient cotransfection was performed on HeLa cells with 2 μg of luciferase and Renilla reporter plasmids using the Amaxa Cell Line Nucleofector Kit R and Amaxa Nucleofector (Lonza). After nucleofection, cells were seeded into wells of a 24-well culture plate for 48 h. Then, NF-κB was induced by incubation of cells with TNF (10 ng/mL) and IFN-γ (100 U) for 6 h. For the induction of AP-1, cells were washed with PBS and cultured in medium without antibiotics and FBS for 4 h. Next, ionomycin (1 μM) was added for 6 h of incubation. To evaluate the influence of **19a** on NF-κB, and AP-1 activity cells were incubated with TNF, IFN-γ, and **19a** or with ionomycin and **19a**. After 6 h of incubation, the cells were harvested and lysed in PLB buffer (Promega). Both firefly and Renilla luciferase activities were assayed with the dual luciferase assay kit (Promega), and the firefly luciferase activities were normalized to activities of Renilla enzyme in each sample. The light emission was determined with GloMax luminometer (Promega). All experiments were repeated at least three times.

4.5.7. ROS Generation Assay. To determine the influence of **19a** on H₂O₂ scavenging activity, HeLa cells were seeded into six-well plates and incubated for 4 h with 10 or 20 μM **19a**. Next, cells were trypsinized, washed, and resuspended in 1 mL of PBS. H₂O₂ at 1 mM final concentration was added to indicated probes for 10 min incubation before staining. One microliter of CM-H₂DCFDA (Invitrogen, 5 mM DMSO solution) was added to each sample for 15 min of incubation at 37 °C. Then, cells were washed twice with PBS and evaluated in flow cytometry using FACSCalibur (Becton Dickinson). For single analysis, 1 × 10⁴ cells were used. Data were analyzed with CELLQuest 1.2 software (Becton Dickinson).

4.5.8. Mice, Tumor Treatment, and Monitoring. BALB/c mice, 8–12 weeks of age, were used in the experiments. Breeding pairs were obtained from the Animal House of the Polish Academy of Sciences, Medical Research Center (Warsaw, Poland). Mice were inoculated subcutaneously with 3.5 × 10⁵ EMT6 cells into the depilated right thigh. Local tumor growth was determined with calipers by the formula: tumor volume (mm³) = (longer diameter) × (shorter diameter)²/2. When tumors reached a longer diameter of 5–7 mm (day 7 of the experiment), the intraperitoneal administration of Trx inhibitors was started and continued for 6 consecutive days. Three groups of mice received investigated compounds—**3** at a dose of 14 mg/kg, **19a** at a dose of 40 mg/kg (equimolar to 14 mg/kg of **3**), or 80 mg/kg. The control group received ip DMSO injection, which was a solvent for all inhibitors. All in vivo experiments were performed in accordance with the guidelines approved by the Ethical Committee of the Medical University of Warsaw.

4.6. Stability Studies. Stock solutions (30 μL, initial concentration: 5 mg/mL) prepared in DMSO were diluted with 3.0 mL of

culture medium or PBS preincubated in 37 °C. After vortexing, the aliquots 100 μL were diluted with 200 μL of 96% ethanol, cooled for 15 min at 4 °C, centrifuged (10000g, 5 min), and stored at –20 °C before the analysis. Residual solutions were incubated at 37 °C up to 7 days. All samples were analyzed using RP-HPLC (C-18 Kromasil column, eluent: acetonitrile:water, PDA detector, method 1 for **19a**, *t_R* = 10.2 min, and method 2 for **3**, *t_R* = 5.9 min, and **2**, *t_R* = 5.1 min). Standard curves were determined with minimum of five dilutions of each compound, prepared as described above. Data points were measured in triplicate in individual experiments (*n* = 3).

■ ASSOCIATED CONTENT

§ Supporting Information

Experimental procedures and spectral data for **6a,6**, **11**, **12**, **16d,e**, and **18a,b**. This material is available free of charge via the Internet at <http://pubs.acs.org>.

■ AUTHOR INFORMATION

Corresponding Author

*Tel: +48 22 5992199. E-mail: jakub.golab@wum.edu.pl (J.G.).
Tel: +48 22 343 2120. E-mail: rysza@icho.edu.pl (R.O.).

Author Contributions

§These authors contributed equally to this work.

■ ACKNOWLEDGMENTS

This work was supported by project “Biotransformations for pharmaceutical and cosmetics industry” No. POIG.01.03.01-00-158/09-07 part-financed by the European Union within the European Regional Development Fund. The author's research was supported by Ministry of Science and Higher education grants N N405 3202 33 (J.G.), N N405 127640 (A.M.), and IP2010 009170 (M.F.). J.G., A.M., and M.F. are members of TEAM Programme cofinanced by the Foundation for Polish Science and the EU European Regional Development Fund. J.G. is a recipient of the Mistrz Award from the Foundation for Polish Science. We thank professor Dieter Seebach from ETH Zürich for valuable suggestions to the mechanism of Trx/TrxR inhibition.

■ DEDICATION

This paper is dedicated to Prof. Janusz Jurczak on the occasion of his 70th birthday.

■ ABBREVIATIONS

AP-1, activating protein-1; ASK1, apoptosis signal-regulating kinase 1; DCM, dichloromethane; DIPEA, di-isopropylethylamine; DMAP, 4-(dimethylamino)pyridine; DMBA, 2,4-dimethoxybenzylamine; DMSO, dimethylsulfoxide; DTT, dithiothreitol; hPBMC, human peripheral blood mononuclear cells; HR-MS, high-resolution mass spectrometry; IFN, interferon; IPTG, isopropyl β-D-1-thiogalactopyranoside; MAP, mitogen-activated protein; mBM, murine bone marrow; MEF, mouse embryonic fibroblasts; MMP, matrix metalloproteinase; NADPH, nicotinamide adenine dinucleotide phosphate; NF-κB, nuclear factor κB; NMR, nuclear magnetic resonance; PBS, phosphor-buffered saline; PTEN, phosphatase and tensin homologue deleted on chromosome ten; ROS, reactive oxygen species; SAHA, suberoyl anilide hydroxamic acid; TBP2, Trx-binding protein-2; TEA, triethylamine; THF, tetrahydrofuran; TNF, tumor necrosis factor; Trx, thioredoxin; TrxR, thioredoxin reductase; VEGF, vascular endothelial growth factor; XTT, 2,3-Bis(2-methoxy-4-nitro-5-sulphophenyl)-2H-tetrazolium-5-carbox-anilide

REFERENCES

- (1) Wu, C.; Parrott, A. M.; Fu, C.; Liu, T.; Marino, S. M.; Gladyshev, V. N.; Jain, M. R.; Baykal, A. T.; Li, Q.; Oka, S.; Sadoshima, J.; Beuve, A.; Simmons, W. J.; Li, H. Thioredoxin 1-mediated post-translational modifications: Reduction, transnitrosylation, denitrosylation, and related proteomics methodologies. *Antioxid. Redox Signaling* **2011**, *15*, 2565–2604.
- (2) Ueno, M.; Masutani, H.; Arai, R. J.; Yamauchi, A.; Hirota, K.; Sakai, T.; Inamoto, T.; Yamaoka, Y.; Yodoi, J.; Nikaido, T. Thioredoxin-dependent redox regulation of p53-mediated p21 activation. *J. Biol. Chem.* **1999**, *274*, 35809–35815.
- (3) Tonissen, K. F.; Di Trapani, G. Thioredoxin system inhibitors as mediators of apoptosis for cancer therapy. *Mol. Nutr. Food Res.* **2009**, *53*, 87–103.
- (4) Powis, G.; Montfort, W. R. Properties and biological activities of thioredoxins. *Annu. Rev. Pharmacol. Toxicol.* **2001**, *41*, 261–295.
- (5) Lee, S. R.; Yang, K. S.; Kwon, J.; Lee, C.; Jeong, W.; Rhee, S. G. Reversible inactivation of the tumor suppressor PTEN by H₂O₂. *J. Biol. Chem.* **2002**, *277*, 20336–20342.
- (6) Sohn, J.; Rudolph, J. Catalytic and chemical competence of regulation of cdc25 phosphatase by oxidation/reduction. *Biochemistry* **2003**, *42*, 10060–10070.
- (7) Arner, E. S.; Holmgren, A. The thioredoxin system in cancer. *Semin. Cancer Biol.* **2006**, *16*, 420–426.
- (8) Weichsel, A.; Gasdaska, J. R.; Powis, G.; Montfort, W. R. Crystal structures of reduced, oxidized, and mutated human thioredoxins: evidence for a regulatory homodimer. *Structure* **1996**, *4*, 735–751.
- (9) Holmgren, A.; Soderberg, B. O.; Eklund, H.; Branden, C. I. Three-dimensional structure of *Escherichia coli* thioredoxin-S2 to 2.8 Å resolution. *Proc. Natl. Acad. Sci. U.S.A.* **1975**, *72*, 2305–2309.
- (10) Forman-Kay, J. D.; Clore, G. M.; Wingfield, P. T.; Gronenborn, A. M. High-resolution three-dimensional structure of reduced recombinant human thioredoxin in solution. *Biochemistry* **1991**, *30*, 2685–2698.
- (11) Kallis, G. B.; Holmgren, A. Differential reactivity of the functional sulfhydryl groups of cysteine-32 and cysteine-35 present in the reduced form of thioredoxin from *Escherichia coli*. *J. Biol. Chem.* **1980**, *255*, 10261–10265.
- (12) Fritz-Wolf, K.; Kehr, S.; Stumpf, M.; Rahlfs, S.; Becker, K. Crystal structure of the human thioredoxin reductase-thioredoxin complex. *Nat. Commun.* **2011**, *2*, 383.
- (13) Chew, E. H.; Lu, J.; Bradshaw, T. D.; Holmgren, A. Thioredoxin reductase inhibition by antitumor quinols: A quinol pharmacophore effect correlating to antiproliferative activity. *FASEB J.* **2008**, *22*, 2072–2083.
- (14) Stadtman, E. R.; Moskovitz, J.; Berlett, B. S.; Levine, R. L. Cyclic oxidation and reduction of protein methionine residues is an important antioxidant mechanism. *Mol. Cell. Biochem.* **2002**, *234*–*235*, 3–9.
- (15) Das, K. C.; Das, C. K. Thioredoxin, a singlet oxygen quencher and hydroxyl radical scavenger: redox independent functions. *Biochem. Biophys. Res. Commun.* **2000**, *277*, 443–447.
- (16) Benhar, M.; Forrester, M. T.; Hess, D. T.; Stamler, J. S. Regulated protein denitrosylation by cytosolic and mitochondrial thioredoxins. *Science* **2008**, *320*, 1050–1054.
- (17) Saitoh, M.; Nishitoh, H.; Fujii, M.; Takeda, K.; Tobiume, K.; Sawada, Y.; Kawabata, M.; Miyazono, K.; Ichijo, H. Mammalian thioredoxin is a direct inhibitor of apoptosis signal-regulating kinase (ASK) 1. *EMBO J.* **1998**, *17*, 2596–2606.
- (18) Mitchell, D. A.; Morton, S. U.; Fernhoff, N. B.; Marletta, M. A. Thioredoxin is required for S-nitrosation of procaspase-3 and the inhibition of apoptosis in Jurkat cells. *Proc. Natl. Acad. Sci. U.S.A.* **2007**, *104*, 11609–11614.
- (19) Biaglow, J. E.; Miller, R. A. The thioredoxin reductase/thioredoxin system: Novel redox targets for cancer therapy. *Cancer Biol. Ther.* **2005**, *4*, 6–13.
- (20) Kakolyris, S.; Giatromanolaki, A.; Koukourakis, M.; Powis, G.; Souglakos, J.; Sivridis, E.; Georgoulas, V.; Gatter, K. C.; Harris, A. L. Thioredoxin expression is associated with lymph node status and prognosis in early operable non-small cell lung cancer. *Clin. Cancer Res.* **2001**, *7*, 3087–3091.
- (21) Raffel, J.; Bhattacharyya, A. K.; Gallegos, A.; Cui, H.; Einspahr, J. G.; Alberts, D. S.; Powis, G. Increased expression of thioredoxin-1 in human colorectal cancer is associated with decreased patient survival. *J. Lab. Clin. Med.* **2003**, *142*, 46–51.
- (22) Powis, G.; Kirkpatrick, D. L.; Angulo, M.; Baker, A. Thioredoxin redox control of cell growth and death and the effects of inhibitors. *Chem.-Biol. Interact.* **1998**, *111–112*, 23–34.
- (23) Welsh, S. J.; Bellamy, W. T.; Briehl, M. M.; Powis, G. The redox protein thioredoxin-1 (Trx-1) increases hypoxia-inducible factor 1α protein expression: Trx-1 overexpression results in increased vascular endothelial growth factor production and enhanced tumor angiogenesis. *Cancer Res.* **2002**, *62*, 5089–5095.
- (24) Farina, A. R.; Tacconelli, A.; Cappabianca, L.; Masciulli, M. P.; Holmgren, A.; Beckett, G. J.; Gulino, A.; Mackay, A. R. Thioredoxin alters the matrix metalloproteinase/tissue inhibitors of metalloproteinase balance and stimulates human SK-N-SH neuroblastoma cell invasion. *Eur. J. Biochem.* **2001**, *268*, 405–413.
- (25) Kim, S. J.; Miyoshi, Y.; Taguchi, T.; Tamaki, Y.; Nakamura, H.; Yodoi, J.; Kato, K.; Noguchi, S. High thioredoxin expression is associated with resistance to docetaxel in primary breast cancer. *Clin. Cancer Res.* **2005**, *11*, 8425–8430.
- (26) Wang, J.; Kobayashi, M.; Sakurada, K.; Imamura, M.; Moriuchi, T.; Hosokawa, M. Possible roles of an adult T-cell leukemia (ATL)-derived factor/thioredoxin in the drug resistance of ATL to adriamycin. *Blood* **1997**, *89*, 2480–2487.
- (27) Yamada, M.; Tomida, A.; Yoshikawa, H.; Taketani, Y.; Tsuruo, T. Increased expression of thioredoxin/adult T-cell leukemia-derived factor in cisplatin-resistant human cancer cell lines. *Clin. Cancer Res.* **1996**, *2*, 427–432.
- (28) Yokomizo, A.; Ono, M.; Nanri, H.; Makino, Y.; Ohga, T.; Wada, M.; Okamoto, T.; Yodoi, J.; Kuwano, M.; Kohno, K. Cellular levels of thioredoxin associated with drug sensitivity to cisplatin, mitomycin C, doxorubicin, and etoposide. *Cancer Res.* **1995**, *55*, 4293–4296.
- (29) Kirkpatrick, D. L.; Kuperus, M.; Dowdeswell, M.; Potier, N.; Donald, L. J.; Kunkel, M.; Berggren, M.; Angulo, M.; Powis, G. Mechanisms of inhibition of the thioredoxin growth factor system by antitumor 2-imidazolyl disulfides. *Biochem. Pharmacol.* **1998**, *55*, 987–994.
- (30) Welsh, S. J.; Williams, R. R.; Birmingham, A.; Newman, D. J.; Kirkpatrick, D. L.; Powis, G. The thioredoxin redox inhibitors 1-methylpropyl 2-imidazolyl disulfide and pleurotin inhibit hypoxia-induced factor 1α and vascular endothelial growth factor formation. *Mol. Cancer Ther.* **2003**, *2*, 235–243.
- (31) Ramanathan, R. K.; Kirkpatrick, D. L.; Belani, C. P.; Friedland, D.; Green, S. B.; Chow, H. H.; Cordova, C. A.; Stratton, S. P.; Sharlow, E. R.; Baker, A.; Dragovich, T. A Phase I pharmacokinetic and pharmacodynamic study of PX-12, a novel inhibitor of thioredoxin-1, in patients with advanced solid tumors. *Clin. Cancer Res.* **2007**, *13*, 2109–2114.
- (32) Powis, G.; Wipf, P.; Lynch, S. M.; Birmingham, A.; Kirkpatrick, D. L. Molecular pharmacology and antitumor activity of palmarumycin-based inhibitors of thioredoxin reductase. *Mol. Cancer Ther.* **2006**, *5*, 630–636.
- (33) Wipf, P.; Hopkins, T. D.; Jung, J. K.; Rodriguez, S.; Birmingham, A.; Southwick, E. C.; Lazo, J. S.; Powis, G. New inhibitors of the thioredoxin-thioredoxin reductase system based on a naphthoquinone spiroketal natural product lead. *Bioorg. Med. Chem. Lett.* **2001**, *11*, 2637–2641.
- (34) Rigobello, M. P.; Scutari, G.; Folda, A.; Bindoli, A. Mitochondrial thioredoxin reductase inhibition by gold(I) compounds and concurrent stimulation of permeability transition and release of cytochrome c. *Biochem. Pharmacol.* **2004**, *67*, 689–696.
- (35) Engman, L.; Al-Maharik, N.; McNaughton, M.; Birmingham, A.; Powis, G. Thioredoxin reductase and cancer cell growth inhibition by organotellurium antioxidants. *Anticancer Drugs* **2003**, *14*, 153–161.
- (36) Bradshaw, T. D.; Matthews, C. S.; Cookson, J.; Chew, E. H.; Shah, M.; Bailey, K.; Monks, A.; Harris, E.; Westwell, A. D.; Wells, G.;

Laughton, C. A.; Stevens, M. F. Elucidation of thioredoxin as a molecular target for antitumor quinols. *Cancer Res.* **2005**, *65*, 3911–3919.

(37) Butler, L. M.; Zhou, X.; Xu, W. S.; Scher, H. I.; Rifkind, R. A.; Marks, P. A.; Richon, V. M. The histone deacetylase inhibitor SAHA arrests cancer cell growth, up-regulates thioredoxin-binding protein-2, and down-regulates thioredoxin. *Proc. Natl. Acad. Sci. U.S.A.* **2002**, *99*, 11700–11705.

(38) Fang, J.; Lu, J.; Holmgren, A. Thioredoxin reductase is irreversibly modified by curcumin: A novel molecular mechanism for its anticancer activity. *J. Biol. Chem.* **2005**, *280*, 25284–25290.

(39) Wipf, P.; Lynch, S. M.; Birmingham, A.; Tamayo, G.; Jimenez, A.; Campos, N.; Powis, G. Natural product based inhibitors of the thioredoxin-thioredoxin reductase system. *Org. Biomol. Chem.* **2004**, *2*, 1651–1658.

(40) Pallis, M.; Bradshaw, T. D.; Westwell, A. D.; Grundy, M.; Stevens, M. F.; Russell, N. Induction of apoptosis without redox catastrophe by thioredoxin-inhibitory compounds. *Biochem. Pharmacol.* **2003**, *66*, 1695–1705.

(41) Davioud-Charvet, E.; McLeish, M. J.; Veine, D. M.; Giegel, D.; Arscott, L. D.; Andricopulo, A. D.; Becker, K.; Muller, S.; Schirmer, R. H.; Williams, C. H. Jr.; Kenyon, G. L. Mechanism-based inactivation of thioredoxin reductase from *Plasmodium falciparum* by Mannich bases. Implication for cytotoxicity. *Biochemistry* **2003**, *42*, 13319–13330.

(42) PCT Int. Appl. WO 2000006088 A2 20000210, 2000.

(43) Holmgren, A. Reduction of disulfides by thioredoxin. Exceptional reactivity of insulin and suggested functions of thioredoxin in mechanism of hormone action. *J. Biol. Chem.* **1979**, *254*, 9113–9119.

(44) Gante, J. Peptidomimetics—Tailored enzyme inhibitors. *Angew. Chem., Int. Ed.* **1994**, *33*, 1699–1720.

(45) Mroczkiewicz, M.; Winkler, K.; Nowis, D.; Placha, G.; Golab, J.; Ostaszewski, R. Studies of the synthesis of all stereoisomers of MG-132 proteasome inhibitors in the tumor targeting approach. *J. Med. Chem.* **2010**, *53*, 1509–1518.

(46) Ralbovsky, L. J.; Scola, M. P.; Sugino, E.; Burgos-Garcia, C.; Weinreb, M. S.; Parves, M. An attempted total synthesis of lysergic acid via an alkene/N-sulfonylimine cyclization. *Heterocycles* **1996**, *43*, 1497–1512.

(47) Obrecht, R.; Herrmann, R.; Ugi, I. Isocyanide synthesis with phosphoryl chloride and diisopropylamine. *Synthesis* **1985**, *4*, 400–402.

(48) Mitra, S.; Lawton, R. G. Reagents for the crosslinking of proteins by equilibrium transfer alkylation. *J. Am. Chem. Soc.* **1979**, *101*, 3097–3110.

(49) Greef de, M.; Abeln, S.; Belkasm, K.; Dömling, A.; Orru, V. A. R.; Wessjohann, A. L. Rapid combinatorial access to macrocyclic ansapeptoids and ansapeptides with natural-product-like core structures. *Synthesis* **2006**, *23*, 3997–4004.

(50) Wagner, B. M.; Smith, R. A.; Coles, P. J.; Copp, L. J.; Ernest, M. J.; Krantz, A. In vivo inhibition of cathepsin B by peptidyl (acyloxy)methyl ketones. *J. Med. Chem.* **1994**, *37*, 1833–1840.

(51) Kirkpatrick, D. L.; Jimale, M. L.; King, K. M.; Chen, T. Synthesis and evaluation of imidazolyl disulfides for selective cytotoxicity to hypoxic EMT6 tumor cells in vitro. *Eur. J. Med. Chem.* **1992**, *27*, 33–37.

(52) Filipek, R.; Rzychon, M.; Oleksy, A.; Gruca, M.; Dubin, A.; Potempa, J.; Bochtler, M. The Staphostatin-staphopain complex: A forward binding inhibitor in complex with its target cysteine protease. *J. Biol. Chem.* **2003**, *278*, 40959–40966.